High-precision narrow-band optical filters for global observation

Atsuo Kurokawa, Yasuhiro Nakajima, Shinji Kimura, Hiroshi Atake, Showa Optronics Co., Ltd. (Japan)
Yoshihiko Okamura, Kazuhiro Tanaka, Japan Aerospace Exploration Agency (Japan)
Shunji Tsuida, Kenichi Ichida, Takahiro Amano, NEC TOSHIBA Space Systems, Ltd. (Japan)
E-mail:a-kurokawa@soc-ltd.co.jp

ABSTRACT

Earth observation satellites are launched to monitor global and long-term climate change, water circulation, and other phenomena. These observations also help increase the accuracy of predictions of environmental changes. Optical band-pass filters that have narrow transmission bands corresponding to specific radiation wavelengths ranging from the near ultraviolet (UV) to infrared (IR) are used for sensor observations. To improve the measurement precision, the required specifications for observation systems including optical band-pass filters are becoming more stringent. The Second-generation Global Imager (SGLI) on the Global Change Observation Mission-Climate (GCOM-C) is a multiband optical imaging radiometer. The optical band-pass filters used for such imagers must have a highly uniform center wavelength (CWL). This paper examines the relationship between the geometry of the substrate fixture and variations in the film thickness on the substrate. A CWL uniformity of better than 0.1% peak-to-peak (pp) in an area of 100 mm × 1 mm is achieved. In addition, it is shown that the CWL shift due to the telecentric error, or the inclination angle of the chief ray in image space, can be compensated for by controlling a filter's CWL distribution.

Keywords: band-pass filter, narrow transmission band, film thickness, uniformity, telecentric

I. INTRODUCTION

The Global Change Observation Mission (GCOM) is the Japan Aerospace Exploration Agency's next Earth environmental observation mission; it consists of the GCOM-W and GCOM-C satellites series for monitoring carbon, water cycles, and climate change [1]. The GCOM-W1 that was launched in May 2012 carries the Advanced Microwave Scanning Radiometer 2, a microwave sensor; it is not discussed in detail here. The GCOM-C1 will carry the Second-generation Global Imager (SGLI) [2, 3], an optical sensor in the wavelength range from the near ultraviolet (UV) to thermal infrared (TIR).

The components of the SGLI are listed in Table 1. The SGLI Visible and Near Infrared Radiometer (VNR) has the important mission of observing land aerosols, vegetation biomass, and other targets with high accuracy to improve sub-processes in numerical climate models. For this reason, high precision of the band-pass filters used for the line sensors is demanded.

Table 2 lists the main specifications of the SGLI-VN filters, which should be fulfilled over an effective area of 82 mm × 1 mm on a substrate. These types of filters are usually realized by optical coatings and designed as interference filters with a dielectric multilayer.

The signal-to-noise ratio can be increased by optimizing each transmission bandwidth, which would make SGLI-VN capable of more precise measurement. This requires both a high central wavelength (CWL) precision and high relative CWL uniformity over the entire effective area of the substrate.

This paper mainly discusses the issues in manufacturing VN filters to meet these demanding specifications and how to fabricate them with simpler methods.

Table 1 Components of SGLI

	Sensors		Monitoring range	Polarization
SGLI	VNR	VN : Visible&Near infrared	380.0-868.5 nm	Unpolarized
		P : Polarimetry	673.5-868.5 nm	P-polarized
	IRS	SW : Shortwave infrared	1050-2210 nm	Unpolarized
		T : Thermal infrared	10.8-12.0 μ m	Unpolarized

II. STRUCTURE OF SGLI-VN FILTER MODULE

The VN filter module is being developed for highly precise observations. Therefore, it is very important not only to realize the specifications in Table 2 but also to suppress stray light in the optical system to low levels, i.e., less than 0.3% of the observation light intensity. However, multiple reflections caused by the surface reflection of lenses, VN filters, and line CCD sensors cause stray light to appear and degrade the observation precisions. In particular, VN filters have enormously high reflectance because they are fabricated using multilayer thin film coatings that reflect unwanted light instead of absorbing it.

To reduce stray light, it is extremely effective to incline the VN filters by 10° or more to the plane normal to the chief ray so that the inner wall of the chassis absorbs the reflected light from each element. However, because the VN filters are intended for the observation of unpolarized light, their polarization sensitivity must be less than 0.5%. Calculations revealed that the maximum inclination of the VN filters is 4°.

For these reasons, the stop band function for each VN filter is provided by V filters and F filters, which reject the light relatively close to and far from the passband region, respectively. In addition, colored glass filters are used as substrates for almost every filter to cut the shorter wavelength range. For example, the spectral characteristics of the V9, F5, and VN9 filters are shown in Fig. 1.

Table 2 Main specifications for passband characteristics of SGLI-VN filters

		unit	VN1	VN2	VN3	VN4	VN5	VN6	VN7	VN8	VN9	VN10	VN11
Center Wavelength (CWL)	Nominal value	nm	380.0	412.0	443.0	490.0	530.0	565.0	673.5	673.5	763.0	868.5	868.5
	Tolerance	nm	±1.5	±1.6	±0.9	±1.0	±1.1	±2.3	±1.3	±1.3	±1.5	±1.7	±1.7
		%	±0.4	±0.4	±0.2	±0.2	±0.2	±0.4	±0.2	±0.2	±0.2	±0.2	±0.2
	Uniformity	nmPP	0.7	0.7	1.1	1.2	1.3	1.0	1.6	1.6	1.4	2.1	2.1
		%PP	0.18	0.18	0.24	0.24	0.24	0.18	0.24	0.24	0.18	0.24	0.24
Band width	FWHM	nm	10	10	10	10	20	20	20	20	12	20	20
	Tolerance	nm	±1.0	±1.0	±1.0	±1.0	±2.0	±2.0	±2.0	±2.0	±1.0	±2.0	±2.0

※Stop-band range is 300–1100 nm.

The VN9 filter consists of V9 filter and F5 filter to meet its specifications. The other VN filters have similar components.
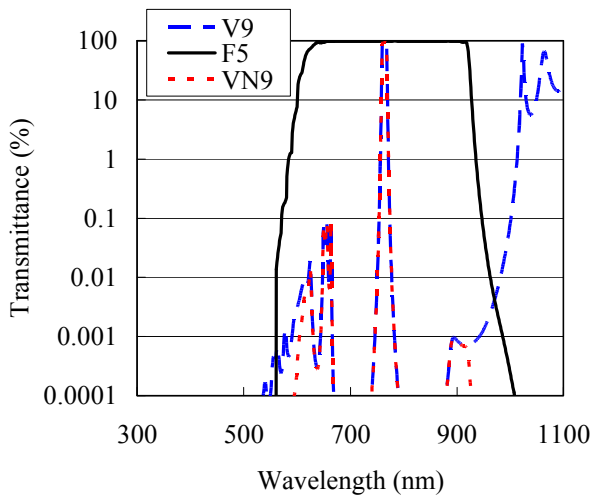
Fig. 1 Spectral characteristics of V9, F5 and VN9 filters

Because the stop band of the F filter is far from the observation wavelength range, the VN filter's polarization characteristics are not greatly affected even if a large inclination angle is applied. Therefore, inclination angles of 10° and 4° were chosen for the F and V filters, respectively. A calculation assuming this configuration showed that the amount of stray light, which was 10% in the first design, could be suppressed to less than 0.1%. The configuration of the optical filter unit is shown in Fig. 2.
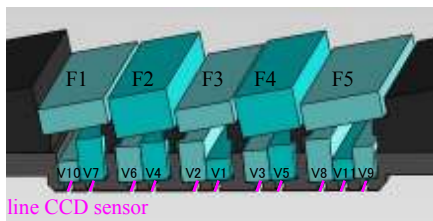
Fig. 2 Schematic diagram of optical filter unit

III. DESIGN OF OPTICAL INTERFERENCE FILTER

The V filters are designed as interference filters with dielectric multilayer. This section provides a brief description of an interference filter.

One of the most basic design formulas for a single-cavity interference filter that has only one Fabry–Perot cavity can be written as follows [4]:

Glass | $(HL)^i$ $2mH$ $(LH)^i$ | Glass
or
Glass | $H(LH)^j$ $2mL$ $(HL)^j$ H | Glass,

where H and L stand for high and low refractive index materials with quarter-wave optical thickness (QWOT) at the design wavelength, and m is an integer.

"$(HL)^i$ $2mH$ $(LH)^i$" and "$H(LH)^j$ $2mL$ $(HL)^j$ H" are referred to as the cavity; examples are shown in Fig.3. In this paper, Ta_2O_5 and SiO_2 were used for the high and low refractive index materials, respectively.

a)

b)
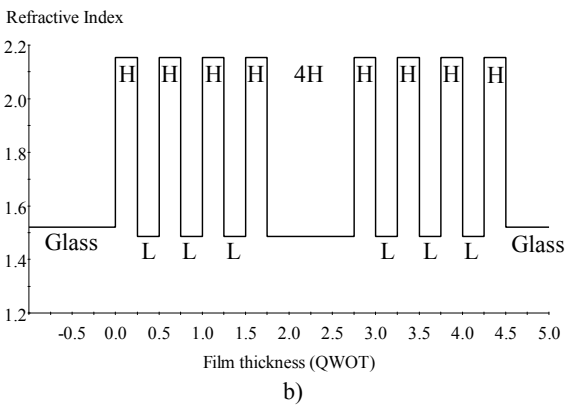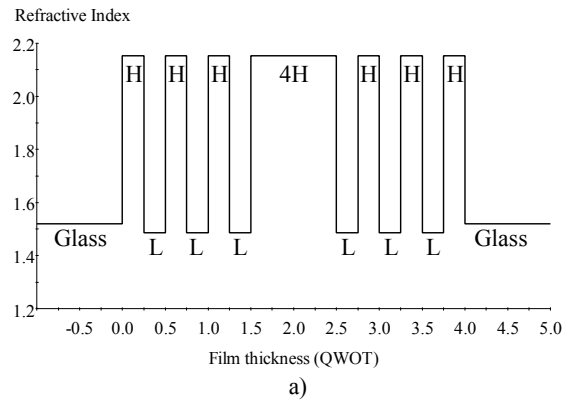
Fig. 3 Index profiles of single cavity interference filters: a) $(HL)^3$ $4H$ $(LH)^3$, b) $H(LH)^3$ $4L$ $(HL)^3$ H

The design of double-cavity and triple-cavity interference filters is represented as follows. The transmission band approaches a rectangle as the number of cavities increases (Fig. 4).

Double-cavity design: Glass | Cavity L Cavity | Glass

Triple-cavity design: Glass | Cavity L Cavity L Cavity | Glass

Here, "Cavity" stands for "$(HL)^3$ $2H$ $(LH)^3$" The high and low refractive index materials are Ta_2O_5 and SiO_2, respectively, and the design wavelength is 532 nm.
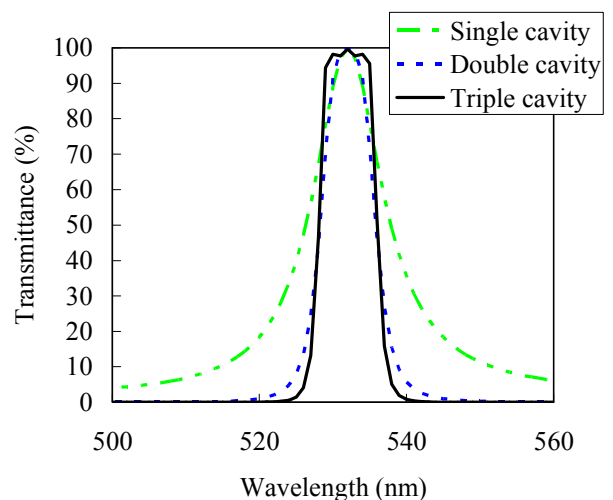
Fig. 4 Spectrum of transmission band for different numbers of cavities

The V filters were designed by triple or quadruple cavity. As an example, the design of the V9 filter that was actually used in this project is as follows. (Its spectrum is shown in Fig. 1).

Colored glass filter
H
$(LH)^3$ 2LH $(LH)^3$
$(LH)^4$ 2LH $(LH)^4$
$(LH)^4$ 2LH $(LH)^4$
$(LH)^3$ 2LH $(LH)^3$
L
Air

H and L stand for Ta_2O_5 and SiO_2, respectively, and the design wavelength is 763 nm.

Various coating methods are used to produce an optical thin film. If an interference filter is fabricated by thermal evaporation, its spectrum shifts to longer or shorter wavelengths depending on the environment because of its porosity [5-7]. To avoid this spectral shift, a dense film is needed; it can be fabricated by ion bombardment or sputtering methods, which increase the particle mobility [8-10]. Because a dense film generally has a high internal compressive stress (greater than 250 MPa), the substrates may be bent when the film become thick. Therefore, to reduce substrate bending, the V filters were designed to have similar film thicknesses on the front and back sides of the substrate.

IV. PRELIMINARY STUDY OF FILM THICKNESS UNIFORMITY

Before the preliminary study, we first decided to adopt plasma ion-assisted deposition (PIAD) as the coating method to produce dense films in this project. Even if a suitable design, material, and coating method are chosen, further difficulties must be overcome to manufacture practical coatings. The most important challenge is to control the film thickness uniformity on the effective area on the substrate. The lack of uniformity causes a shift in the spectral characteristics across the substrate. That is to say, it is an error of the relative CWL uniformity.

The basic equation for estimating the film thickness uniformity in the evaporation process can be written as follows [11, 12]:

$$t = (m/\pi\mu) \times \cos\theta\cos\varphi/r^2. \tag{1}$$

where t is the layer thickness, m is the total mass of materials emitted from the source in all directions, μ is the film density, and r is the distance between the evaporation source and P (x, y, z) that is an arbitrary point on the substrate. θ is the angle between the normal to the surface of the source and direction from the source to the P. Further, φ is the angle between the normal to the surface of the substrate and direction from the P to the source.

Prior to actual calculation of the film thickness, the location of the substrate need to be determined. There are two types of substrate holder that are commonly used in the evaporation process. One is a spherical holder and the other is a flat holder [Fig. 5 and 6].

For a flat substrate holder, when the height of the substrate above the source is set to h, r is given by $h/\cos\theta$ and φ equals θ. Then, the thickness will be simplified as follows:

$$t = (m/\pi\mu) \times \cos^4\theta/h^2. \tag{2}$$

In fact, because arbitrary locations on the substrate differ in θ, φ, and r, a thickness distribution on the substrate occurs. Thus, to estimate the thickness distribution on a substrate before the V filters are manufactured, we calculated the film thickness of arbitrary point P (x, y, z) on a substrate 100 mm × 30 mm in size for a spherical and a flat substrate holders. Each parameter used in the calculation, such as θ, φ, and r, is determined in accordance with the configuration of our equipment (PIAD). A substrate 100 mm × 30 mm in size was used to make the V filters, which were 82 mm × 1 mm in size.
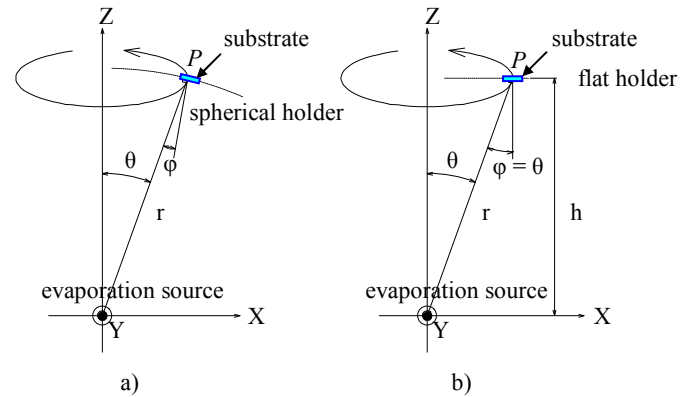
Fig. 5 Comparison of a) spherical and b) flat substrate holders
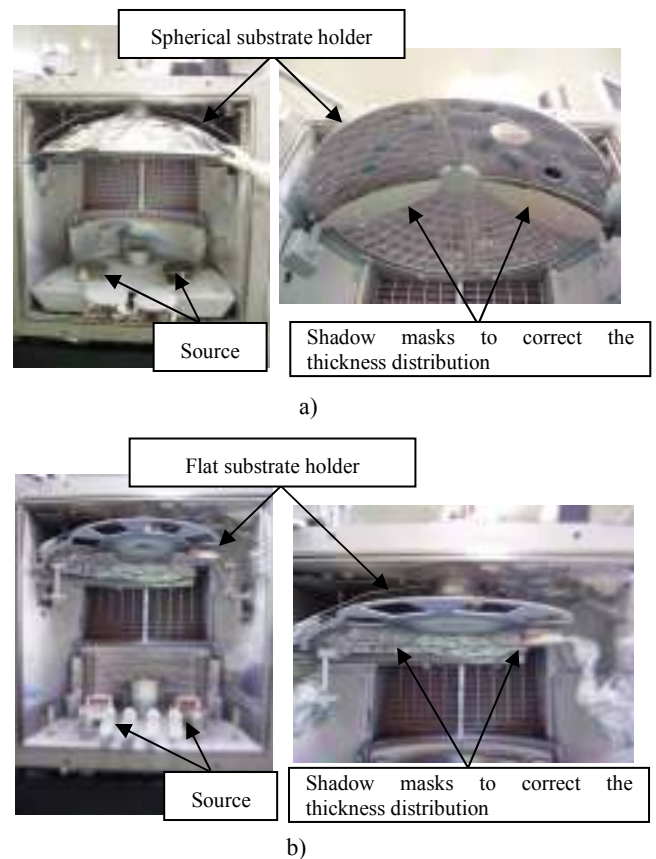
Fig. 6 Equipment (PIAD) with a) spherical and b) flat substrate holders

The calculated peak-to-peak (pp) film thickness uniformity over an area of 100 mm × 30 mm for the spherical holder is 1.3% [Fig. 7(a)], and that for the flat holder is 5.0% [Fig. 7(b)]. In both cases, the relative thickness error is approximately 0.5% along the longer direction of the substrate. This result indicates that neither the spherical holder nor the flat holder meets the specifications for VN filters.
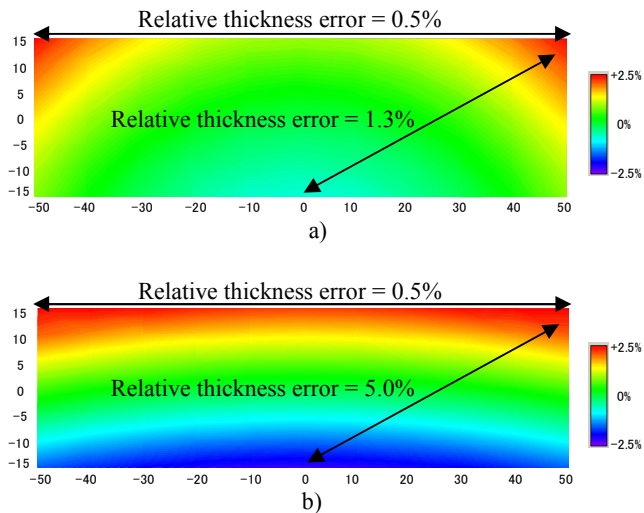
Fig. 7 Relative peak-to-peak thickness error over an area of 100 mm × 30 mm: a) spherical holder without a shadow mask and b) flat holder without a shadow mask

The thickness distribution was recalculated on the basis of the assumption that a shadow mask is used to correct the distribution along the longer direction of the substrate. The recalculated relative thickness error over an area of 100 mm × 30 mm is 4% pp [Fig. 8(a)] for the spherical holder and 0.05% pp [Fig. 8(b)] for the flat holder. These results indicate that it may be possible to manufacture VN filters only when a flat holder is used.
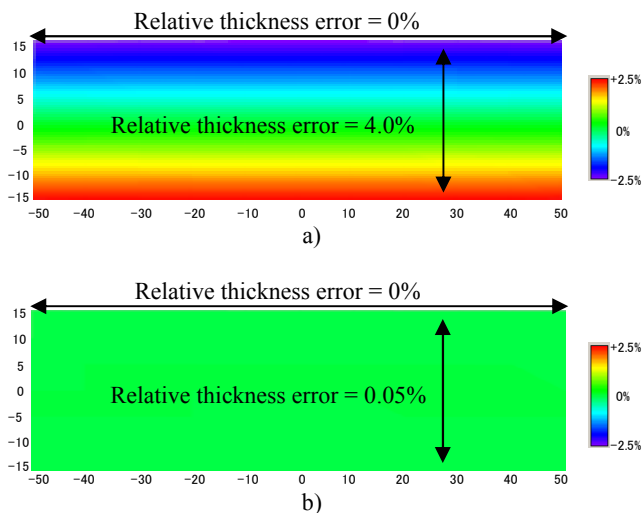
Fig. 8 Relative peak-to-peak thickness error over an area of 100 mm × 30 mm: a) spherical holder with a shadow mask and b) flat holder with a shadow mask

In practice, the thickness distribution on the substrate varied randomly batch-by-batch with slight variations in the shape of the source materials and lack of repeatability of the substrate temperature and degree of vacuum. Therefore, it is impossible to achieve complete uniform film thickness even if a shadow mask with an optimized shape is used.

V. RESULTS AND DISCUSSION

Because the F filters have little effect on the specifications of the transmittance band of the VN filters, maximum errors of up to ±2% can be allowed in the CWL and relative CWL uniformity precisions together. Therefore, the F filters were manufactured by a conventional deposition method. The details are not given here.

The CWL errors of the V filters can be controlled to be better than ±0.1% by a direct optical monitor system, which monitored the actual filter to control the film thickness [13]. The resulting CWL errors are shown in Fig. 9.
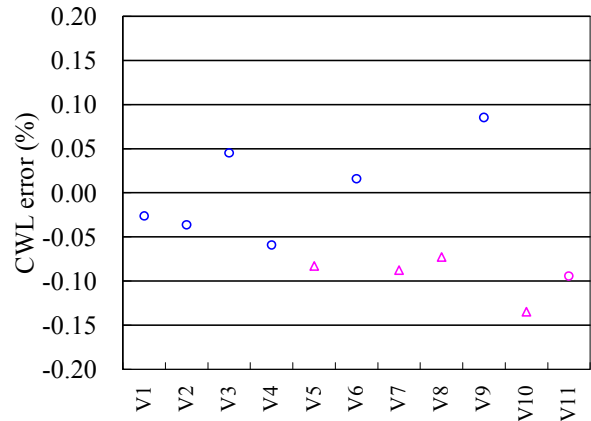
Fig. 9 CWL error of each band (blue circles: manufactured by PIAD, pink triangles, manufactured by the conventional method)

1) CWL uniformity

As mentioned above, the flat holder offers better correction of the thickness distribution on a substrate than the spherical holder. Therefore, the flat holder was used to manufacture the V filters described below.

In the previous section, we assumed that the thickness distribution is proportional to $\cos^4\theta$. However, in the actual coating process, this is not always true because of differences in the source material characteristics. Therefore, the factor $\cos^4\theta$ was replaced by $\cos^x\theta$ in equation 2 to match the true thickness distribution. Then, x was experimentally determined to be 3.0 ± 0.2.

A calculation based on this value of x yields a batch-to-batch relative uniformity of less than 0.04% pp over a substrate area of 82 mm × 1 mm. This margin of error is tolerable in the fabrication of V filters with the required specification of 0.18% pp.

A relative CWL uniformity of 0.18% pp (Fig. 10) was achieved over an area of 82 mm × 1 mm by the method described above using the flat holder and shadow mask with the optimized shape. In addition, a relative CWL uniformity of better than 0.06% pp was achieved over an area of 100 mm × 1 mm along the longer direction of the V1 filter (Fig. 11).
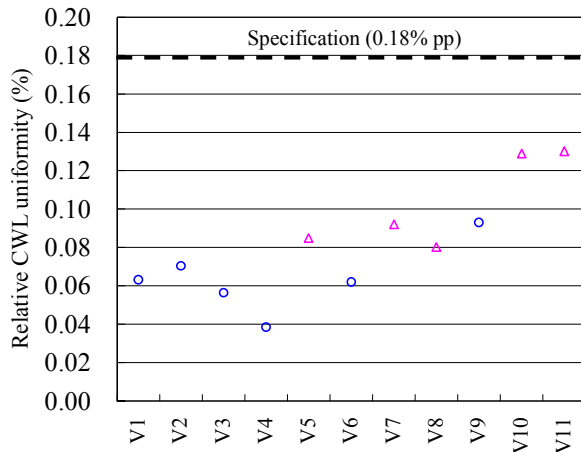
Fig. 10 Relative CWL uniformity of each band (blue circles: manufactured by PIAD, pink triangles: manufactured by the conventional method)
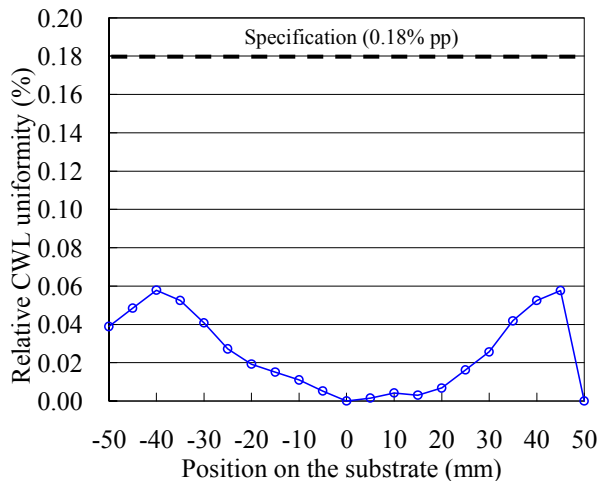
Fig. 11 Relative CWL uniformity along the longer direction of the V1 filter

2) Controlling CWL distribution on substrate

The wavelength characteristics of an interference filter generally shift depending on the incident angle. As the angle of incidence increases, the wavelength characteristics shift to shorter wavelengths.

When an optical system has a telecentric error or the inclination angle of the chief ray in image space, the angle of incidence to the band-pass filter varies the basis of the position on a substrate. In other words, the CWL shift due to the telecentric error of the optical lens should be able to be compensated by controlling film thickness distribution along the longer direction of the substrate.

The shape of the shadow mask used to correct the film thickness distribution in V filter fabrication can be changed easily. Thus, the film thickness distribution over an area of 82 mm × 1 mm, which is the size of the V filters, can be controlled freely using a shadow mask. As a first step of feasibility study of compensating a telecentric error of optical lens, we have demonstrated doubling the film thickness variation along the longer direction of a substrate compared to the V1 filter. As shown in Fig. 12, the CWL variation of the sample was approximately 2.5 times that of the V1 filter.
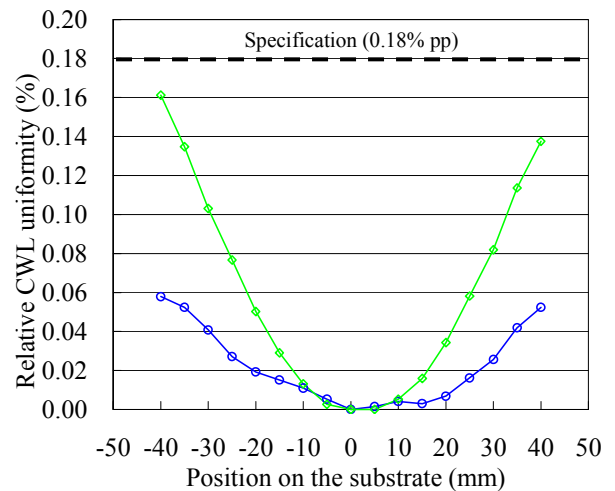
Fig. 12 Control of film thickness distribution. Blue circles: control using a shadow mask to correct the distribution along the longer direction of the substrate, green diamonds: control using a shadow mask to double the variation of the V1 filter

VI. CONCLUSION

In the manufacture of narrow-band optical filters for global satellite observations, a CWL error of better than ±0.1% and a relative CWL uniformity of better than 0.1% pp over an area of 100 mm × 1 mm were achieved. In addition, it was demonstrated that the CWL shift due to a telecentric error, or the inclination angle of the chief ray in image space, can be compensated for by controlling the film thickness distribution on the substrate using a shadow mask. These results were achieved by a simpler method using PIAD and a flat plane substrate holder.

REFERENCES

[1] K. Imaoka, M. Kachi, H. Fujii, H. Murakami, M. Mori, A. Ono, T. Igarashi, K. Nakagawa, T. Oki, Y. Honda and H. Shimoda, *Proc. IEEE* , 2010.

[2] Y. Okamura, K. Tanaka, T. Amano, M. Hiramatsu and K. Shiratama, *Proc. SPIE* **7106,** 2008.

[3] K. Tanaka, Y. Okamura, T. Amano, M. Hiramatsu and K. Shiratama, *Proc. SPIE* **7862,** 2010.

[4] H. A. Macleod, *Thin-Film Optical Filters* (Macmillan, London, 1986) pp.244-257, pp.270-286

[5] J. A. Ruffner, M. D. Himel, V. Mizarahi, G. I. Stegeman and U. J. Gibson, *Appl. Opt.* **28**, 5209, 1989.

[6] S. Mohan and M. G. Krishna, *Vacuum* **46**, 645, 1995.

[7] F. Flory and L. Escoubas, *Progress in Quantum Electronics* **28**, 89, 2004.

[8] J. K. Fu, G. Atanassov, Y. S. Dai, F. H. Tan and Z. Q. Mo, *J. Non-Crys.Solids* **218**, 403, 1997.

[9] G. Atanassov, J. Turlo, J. K. Fu and Y. S. Dai, *Thin Solid Films* **342**, 83, 1999.

[10] D. R. Gibson and C. Huiguang, *45th Annual Technical Conference Proceedings of the Society of Vacuum Coaters* pp.611-615, 2002.

[11] L. Holland and W. Steckelmacher, *Vacuum* **2** 346-64, 1952.

[12] K. H. Behrndt, *10th AVS Nat. Vac. Symp.* (Macmillan, London, 1963) pp.379-84

[13] H. D. Polster, *J. Opt. Soc. Am.* **42** 21-5, 1952.